

Achieving Thresholds via Standalone Belief Propagation on Surface Codes

Pedro Hack,^{1,*} Luca Menti,^{1,†} Francisco Lázaro,^{1,‡} and Alexandru Paler^{2,§}

¹German Aerospace Center, Germany

²Aalto University, Finland

The usual belief propagation (BP) decoders are, in general, exchanging local information on the Tanner graph of the quantum error-correcting (QEC) code and, in particular, are known to not have a threshold for the surface code. We propose novel BP decoders that exchange messages on the decoding graph and obtain code capacity thresholds via standalone BP for the surface code under depolarizing noise. Our approach, similarly to the minimum weight perfect matching (MWPM) decoder, is applicable to any graphlike QEC code. The thresholds observed with our decoders are close to those obtained by MWPM. This result opens the path towards scalable hardware-accelerated implementations of MWPM-compatible decoders.

I. INTRODUCTION

The failure of standard Belief Propagation (BP) to exhibit a threshold for the surface code has long been viewed as a fundamental limitation arising from the highly loopy structure of the code's Tanner graph. In this work, we reconcile the local-update nature of BP with the global topological requirements of surface code decoding. We demonstrate that BP's failure is not an inherent property of the algorithm itself, but rather a consequence of the graph representation onto which the physics of the error model is mapped. By shifting the message-passing dynamics from the syndrome-based Tanner graph to the topological decoding graph, we recover the threshold behavior. This suggests that the lack of convergence previously observed in BP is an extrinsic artifact of the graph construction.

A. Motivation

For graphlike CSS codes, i.e. each qubit error only affects two checks in each parity check matrix, the standard decoding algorithm is minimum weight perfect matching (MWPM). Graphlike CSS codes include several important codes [1–6] such as the surface code. At the same time, graphlike approaches like MWPM can be adapted to more general codes [7–9].

The complexity of a naïve implementation of MWPM scales like $O(n^3 \log n)$, where n is the number of physical qubits. In general, this is considered to be prohibitively slow for decoding large scale fault-tolerant quantum computations, which hence motivates the study of fast MWPM implementations whose performance does not degrade abruptly [10–12].

Herein, we explore the use of standalone BP-based approaches to MWPM as a decoder for quantum error cor-

rection. We present algorithms which save computational time when compared to MWPM by taking a BP approach to the problem, that is, by **running message-passing on the QEC decoding graph**, the same graph where MWPM operates. This contrasts with the standard BP approach to decoding [13, 14], which performs message-passing directly on the QEC code's Tanner graph.

Our algorithms have a slightly higher time complexity than BP and are, similarly to MWPM, restricted to graphlike codes (Sec. II). However, they can significantly improve the performance of BP decoding, and in contrast to vanilla BP [15] which does not achieve threshold, our algorithms are achieving it (Sec. III).

The use of message-passing to obtain matchings was already proposed by [16–20]. However, such approaches were never used for QEC decoding purposes, and very little evidence regarding their practical performance was previously provided. Moreover, they were mostly focused on emulating the behavior of MWPM, while our goal is to test their performance when we constraint their time complexity.

B. MWPM on the surface code

Our BP-based method is applicable as a direct replacement of vanilla MWPM. For simplicity, we focus on uncorrelated decoding in the surface code, and decode X and Z Pauli errors separately. In the following, we fix the case of Z Pauli errors and refer to the X parity check matrix by \mathbf{H} .

When decoding Z errors, MWPM works on the **decoding graph** $\mathcal{G} = (\mathcal{V}, \mathcal{E})$. For each error realization \mathbf{e} , the decoding graph consists of one node $i \in \mathcal{V}$ for each unsatisfied check, as well as one edge $(i, j) \in \mathcal{E}$ for each pair of unsatisfied checks. The edge (i, j) represents the fact that one can map the unsatisfied check associated to i to the one associated to j . Additionally, for each unsatisfied check associated with some vertex $i \in \mathcal{V}$, the decoding graph contains a **boundary node** $i_b \in \mathcal{V}$ and a boundary edge $(i, i_b) \in \mathcal{E}$. The boundary node and the edge represent the fact that one can map the unsatisfied check to the boundary.

* pedro.hack@dlr.de

† luca.menti@dlr.de

‡ francisco.lazaroblasco@dlr.de

§ alexandru.paler@aalto.fi

For a given error realization \mathbf{e} , we will denote by s its associated number of unsatisfied checks. In this scenario, the decoding graph consists of $|\mathcal{V}| = 2s$ and $|\mathcal{E}| = s(s-1)/2 + s$. That is, for a given physical error rate p (in the worst case scenario where the faulty qubits do not share any check with each other) the maximum expected number of unsatisfied checks is $2pn = O(n)$ for large n . As a result, taking into account the boundary vertices, the decoding graph has at most $|\mathcal{V}| = 2pn + 2pn = O(n)$ and $|\mathcal{E}| = 2pn(2pn-1)/2 + 2pn = O(n^2)$. Fig. 1 shows an error realization and its associated decoding graph.

MWPM associates a weight to each edge in the decoding graph and runs the Blossom algorithm [21, 22] in order to find an error \mathbf{e}' with minimal weight that has the observed syndrome $\mathbf{H}\mathbf{e}' = \mathbf{H}\mathbf{e}$. Instead of doing this, we associate a **factor graph** \mathcal{F} to the decoding graph and correct errors by running BP on \mathcal{F} .

II. METHODS

We describe the main subroutines of our algorithms, and discuss their complexity by assuming a parallelized implementation.

Our factor graph $\mathcal{F} = (\mathcal{V} \cup \mathcal{E}, \mathcal{E}')$ has one factor node for each node in the decoding graph and one variable node for each edge in the decoding graph. Additionally, it has an edge between a factor node and a variable node whenever the edge associated to the variable node is incident to the node in \mathcal{G} associated to the factor node.

We denote by $v_1, \dots, v_{s(s-1)/2}$ the variable nodes that are not incident to factors associated to boundary nodes and by u_1, \dots, u_s the rest. The variable nodes take binary values $v_i, u_j \in \{0, 1\}$, and we interpret the **value one to mean that the edge in \mathcal{G} associated to the variable should be included in the matching** and zero to mean the opposite. Moreover, we denote by $x_1, \dots, x_{s(s-1)/2}$ (y_1, \dots, y_s) the values that variables $v_1, \dots, v_{s(s-1)/2}$ (u_1, \dots, u_s) take.

The factor graph \mathcal{F} consists of the following factors:

- Each $i \in \mathcal{V}$ contributes to \mathcal{F} with a factor c_i that takes the form

$$c_i(x_1^i, \dots, x_{s-1}^i, y_i) = \begin{cases} 1 & \text{if } y_i + \sum_{j=1}^{s-1} x_j^i = 1, \\ 0 & \text{else,} \end{cases} \quad (1)$$

where $v_1^i, \dots, v_{s-1}^i, y_i$ are the variable nodes that share an edge in \mathcal{E}' with factor node i .

- Each $i \in \mathcal{E}$ associated to two unsatisfied syndromes i and j contributes to \mathcal{F} with a factor q_{ij} that takes the form:

$$q_{ij}(x_{ij}) = \begin{cases} \left(\frac{p}{1-p}\right)^{w_{ij}} & \text{if } x_{ij} = 1, \\ 1 - \left(\frac{p}{1-p}\right)^{w_{ij}} & \text{if } x_{ij} = 0, \end{cases} \quad (2)$$

where v_{ij} is the variable that connects i and j , and w_{ij} is the weight of the smallest error that matches syndromes i and j .

- Each $i \in \mathcal{E}$ associated to a single unsatisfied syndrome i contributes to \mathcal{F} with a factor q_i that takes the form:

$$q_i(y_i) = \begin{cases} \left(\frac{p}{1-p}\right)^{w_i} & \text{if } y_i = 1, \\ 1 - \left(\frac{p}{1-p}\right)^{w_i} & \text{if } y_i = 0, \end{cases} \quad (3)$$

w_i is the weight of the smallest error that matches syndrome i to the boundary.

Factors associated to unsatisfied syndromes represent the fact that each unsatisfied syndrome should be either matched to another unsatisfied syndrome or to its associated boundary node. Factors associated to variables in \mathcal{G} represent the prior probability that the variable is part of the final matching.

Overall, the factor graph \mathcal{F} represents the probability distribution \mathbb{P}_0 over all the possible combinations of $v_1, \dots, v_{s(s-1)/2}$ and u_1, \dots, u_s :

$$\mathbb{P}_0(x_1, \dots, x_{s(s-1)/2}, y_1, \dots, y_s) \propto \prod_{1 \leq i \leq s} c_i(x_1^i, \dots, x_{s-1}^i, y_i) \prod_{1 \leq j < k \leq s} q_{jk}(x_{jk}) \prod_{1 \leq \ell \leq s} q_\ell(y_\ell) \quad (4)$$

giving zero probability to those not associated to matchings, and distinguishing the matchings in terms of the probability that each of their associated edges is independently taken. We omit a normalization constant in (4).

Finding a minimum weight perfect matching is equivalent to maximizing \mathbb{P}_0 . In order to do so, we run the sum-product belief propagation algorithm on \mathcal{F} . Fig. 1 shows an error realization and its associated factor graph.

A. Message-passing

Our message-passing algorithms send messages from factor to variable nodes and vice versa. If we denote by f a generic factor node and by v a generic variable node then we use the set of messages

$$\left\{ m_{f \rightarrow v}^{(t)}, m_{v \rightarrow f}^{(t)} \right\}_{f \in \mathcal{V}, v \in \mathcal{N}(f), t=0, \dots, T},$$

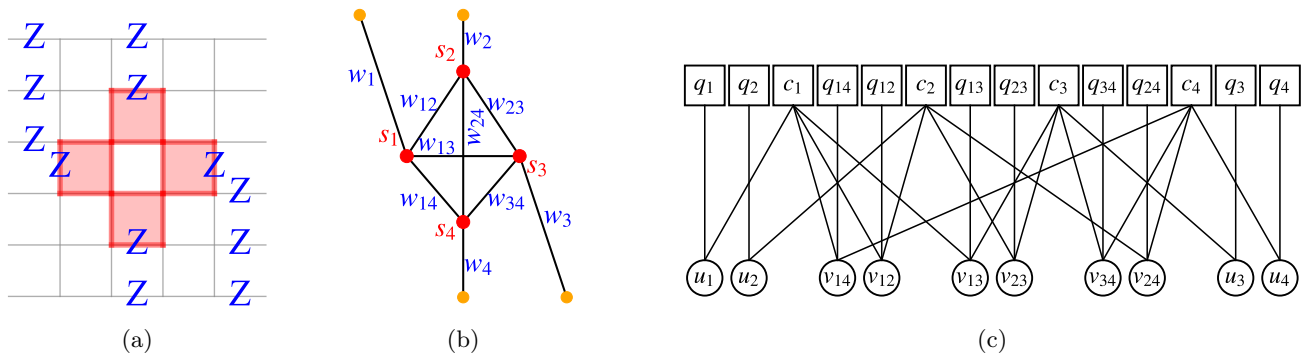


FIG. 1: Decoding and factor graphs. (a) Example error realization e in the $d = 5$ unrotated surface code. Z phase-flip errors are blue and unsatisfied syndrome plaquettes are red. (b) Decoding graph associated to e . The unsatisfied syndromes are associated to red nodes and the boundary nodes are orange. We include one edge for each pair of unsatisfied syndromes and one edge that joins each unsatisfied syndrome to the boundary. Each edge has a weight $w^p \equiv (p/(1-p))^w$ (2) and (3), where p is the physical error rate and w is the weight of the shortest error path that satisfies the syndromes connected by the edge. We abuse the notation in this figure and refer to w^p simply as w . Although the code has only two boundaries, we include four boundary nodes since we use each path from an unsatisfied syndrome to the boundary independently. (c) Factor graph associated to e . Each unsatisfied syndrome i is associated to a factor c_i (1), a factor q_i (3) and a variable u_i . Each pair of unsatisfied syndromes i, j are associated to a factor q_{ij} (2) and a variable v_{ij} .

where $\mathcal{NN}(f)$ are the variable nodes adjacent to f in \mathcal{F} and T is some predefined number of iterations.

The messages from variables to factors $m_{v \rightarrow f}^{(0)}$ are initialized using the prior probability associated to each variable (2) and (3), and the messages from factors to variables $m_{f \rightarrow v}^{(0)}$ are uniformly initialized.

In a naive implementation, the messages are updated as follows:

- If $f \in \{c_1, \dots, c_s\}$, then

$$\begin{aligned}
 m_{f \rightarrow v}^{(t+1)}(1) &\propto \prod_{v' \in \mathcal{NN}(f) \setminus v} m_{v' \rightarrow f}^{(t)}(0), \\
 m_{f \rightarrow v}^{(t+1)}(0) &\propto \sum_{v' \in \mathcal{NN}(f) \setminus v} m_{v' \rightarrow f}^{(t)}(1) \prod_{v'' \in \mathcal{NN}(f) \setminus v, v'} m_{v'' \rightarrow f}^{(t)}(0), \\
 m_{v \rightarrow f}^{(t+1)}(x) &\propto \prod_{f' \in \mathcal{NN}(v) \setminus f} m_{f' \rightarrow v}^{(t)}(x),
 \end{aligned} \tag{5}$$

for $x \in \{0, 1\}$ and $0 \leq t \leq T - 1$.

- If $f \notin \{c_1, \dots, c_s\}$, then we do not update the messages $m_{f \rightarrow v}^{(t+1)}(x) = m_{f \rightarrow v}^{(t)}(x)$ and $m_{v \rightarrow f}^{(t+1)}(x) = m_{v \rightarrow f}^{(t)}(x)$ for $x \in \{0, 1\}$ and $0 \leq t \leq T - 1$.

All messages are renormalized such that

$$\sum_{x=0,1} m_{f \rightarrow v}^{(t+1)}(x) = \sum_{x=0,1} m_{v \rightarrow f}^{(t+1)}(x) = 1$$

for $0 \leq t \leq T - 1$.

At each message-passing iteration of our algorithms we update the messages (5). Since each variable node

has at most three factors adjacent to it, and we can update each of them in parallel, updating variable to factors messages can be done in $O(1)$. The factors, however, are adjacent to $O(n)$ variable nodes. Using the leave-one-out approach [23], we can update each message from a factor node to a variable node in $O(n)$. Since we can do each of them in parallel, each message passing iteration takes $O(n)$.

B. Checking convergence

The algorithm **converged** if we find an error candidate e' with the same syndrome as the actual error $\mathbf{H}e' = \mathbf{H}e$. Checking convergence in our algorithms is useful since there is no guarantee that message-passing will achieve it. Hence, if we check for it early, it may save us computational time.

Assuming that we have inferred an error candidate, checking for convergence requires for each factor node to sum over the inferred values of the variable nodes adjacent to it. If the sum is equal to one for all factor nodes, then we have converged. This can be parallelized for each factor node and, as a result, requires $O(n)$ time.

C. Inference

We infer an error candidate e' by using the set of messages from checks to variables. We consider two inference methods: **marginalization** and **forced convergence**.

In marginalization, we infer the posterior probability distribution $\mathbb{P}^{(t)}(w = x)$ for each individual variable

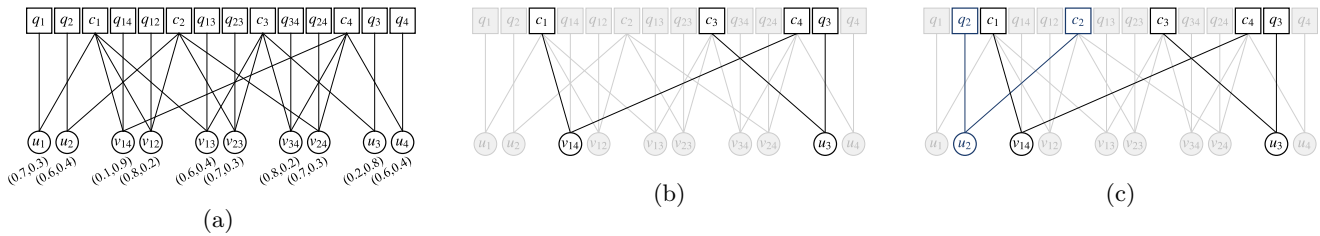


FIG. 2: Marginalization and forced convergence: (a) An example marginalization output ($\mathbb{P}^{(T)}(w=0), \mathbb{P}^{(T)}(w=1)$) for each variable w and the error candidate in Fig. 1; (b) The error candidate provided by marginalization does not converge. (c) The error candidate provided by forced convergence, which always converges.

Name	Iter. Comp.	#Iter.	Non-conv. Ratio	Inf. Comp.	Overall Comp.	Threshold
BP4M- $\log n$	$O(n)$	$O(\log n)$	$0 \leq r_{nc} \leq 1$	$O(n \log n)$	$O(n \log n)$	0.124
BP4M- \sqrt{n}	$O(n)$	$O(\sqrt{n})$	$0 \leq r_{nc} \leq 1$	$O(n \log n)$	$O(n^{3/2})$	0.117
BP4MF- $\log n$	$O(n \log n)$	$O(\log n)$	$r_{nc} = 0$	-	$O(n \log^2 n)$	0.125
BP4MF- \sqrt{n}	$O(n \log n)$	$O(\sqrt{n})$	$r_{nc} = 0$	-	$O(n^{3/2} \log n)$	0.134
BP4M- $\log n + M$	$O(n)$	$O(\log n)$	$0 \leq r_{nc} \leq 1$	$O(r_{nc} n^3 \log n)$	$O((1 - r_{nc})n \log n + r_{nc} n^3 \log n)$	0.157
BP4M- $\sqrt{n} + M$	$O(n)$	$O(\sqrt{n})$	$0 \leq r_{nc} \leq 1$	$O(r_{nc} n^3 \log n)$	$O((1 - r_{nc})n^{3/2} + r_{nc} n^3 \log n)$	0.157

TABLE I: Algorithms' worst case complexity and thresholds. The second column is the complexity per iteration; the second column is the number of iterations; the third column is the proportion of times that BP converges (i.e. finds an error compatible with the syndrome); the fourth column is the complexity of inference after BP (a hyphen indicates that this step is not needed since BP always converges); the fourth column is the overall complexity; the fifth column is the observed code capacity threshold. For standard MWPM the threshold is 0.155 [24]. The complexities reported here are for a parallel implementation (see Section II).

$w \in \{v_1, \dots, v_{s(s-1)/2}, u_1, \dots, u_s\}$ and decide whether to include it in the matching or not based solely on its posterior. Given this local constraint on the decoder's decision, we are not guaranteed to converge. Fig. 4b provides data for the number of times we do not obtain (through marginalization) a converged error candidate in any of the $\log n$ or \sqrt{n} iteration steps.

On the other hand, forced convergence uses the posteriors computed by marginalization for ordering all variable nodes in terms of their probability of being part of the matching. We then recursively pick the variable with the highest probability until we obtain a matching. The serial decision on the variables together with their ordering in terms of likelihood provide global information that always allows us to provide an error candidate matching the syndrome.

1. Marginalization

For each $w \in \{v_1, \dots, v_{s(s-1)/2}, u_1, \dots, u_s\}$ we compute its marginal

$$\mathbb{P}^{(t)}(w=x) \propto \prod_{f \in \mathcal{NN}(w)} m_{f \rightarrow w}^{(t)}(x),$$

where we omit a normalization constant, and include w in the matching provided

$$\mathbb{P}^{(t)}(w=1) > \mathbb{P}^{(t)}(w=0).$$

The marginalization over each variable requires $O(1)$ time since each variable node is only connected to at most three factor nodes. Since we can marginalize each variable in parallel, we only require $O(1)$ time for marginalizing. Fig. 2 is an example where marginalization does not converge.

2. Forced convergence

In order to force the convergence, we can assume that we have associated to each c_i with $i \in \mathcal{V}$ some subset of its adjacent variable nodes

$$\mathcal{E}_i \subseteq \mathcal{NN}(c_i)$$

such that we partition the set of variable nodes in non-intersecting subsets

$$\mathcal{E} = \cup_i \mathcal{E}_i \text{ and } \mathcal{E}_i \cap \mathcal{E}_j = \emptyset.$$

This partition can be pre-computed assuming each syndrome is unsatisfied and obtaining a partition for the complete set of variable nodes that the decoding graph may be. Each \mathcal{E}_i can then be in parallel adapted to the observed syndrome for a total cost of $O(n)$.

Once we have the desired partition, we marginalize each individual variable in $O(1)$ and use this information to compute

$$w_{max}^i \equiv \arg \max_{w \in \mathcal{E}_i} \left\{ \mathbb{P}^{(t)}(w=1) \right\}$$

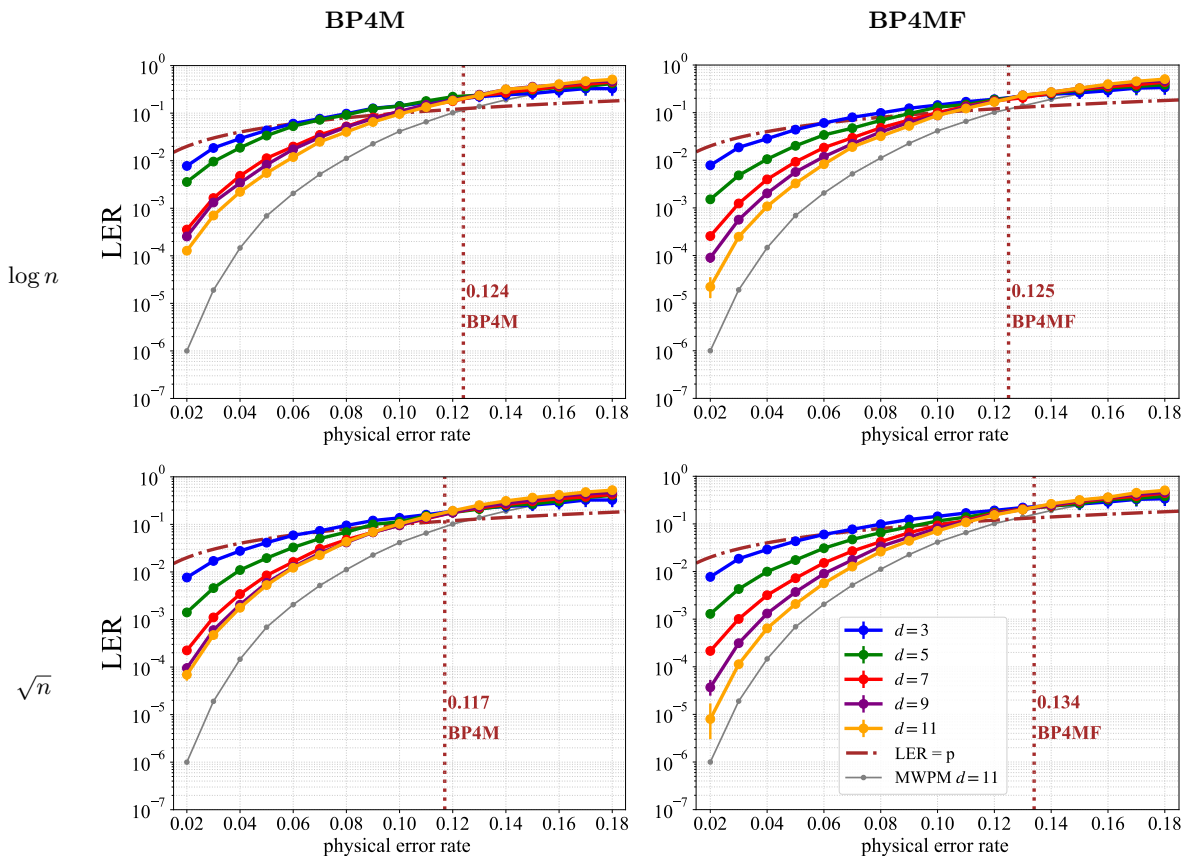


FIG. 3: Threshold plots. The columns determine the algorithm, and the rows are the number of iterations. The horizontal red dotted line is the **pseudo-threshold** (i.e. the curve where the logical error rate equals the physical error rate) and the vertical dotted line indicates the achieved threshold. Our algorithms perform best at high error-rates. All subfigures include a gray LER curve that represents pure MWPM distance 11 decoding performance. This is for comparison reasons with the corresponding distance 11 LER curve of our methods (orange). BP4M’s performance seems to plateau for distances larger than 11, but we can avoid this effect by forcing the convergence and implementing BP4MF, whose decoding performance approaches MWPM.

for each $i \in \mathcal{V}$. Since we can do this for each of them in parallel, this requires $O(n)$.

We then build the vector of maxima $\mathbf{w}_{max} = (w_{max}^1, \dots, w_{max}^s)$ and reorder it \mathbf{w}_{max}^π such that

$$\mathbb{P}^{(t)}((\mathbf{w}_{max}^\pi)_i = 1) \geq \mathbb{P}^{(t)}((\mathbf{w}_{max}^\pi)_{i+1} = 1)$$

for $i = 1, \dots, s - 1$. When performed serially, reordering requires $O(n \log n)$, but there exist parallel hardware implementations [25] with even lower complexity.

As a last step, we go over \mathbf{w}_{max}^π in ascending variable order and, at every time step, we take the first element $(\mathbf{w}_{max}^\pi)_1$ and we remove it from \mathbf{w}_{max}^π (together with possibly another location $(\mathbf{w}_{max}^\pi)_j$ provided the variable associated to $(\mathbf{w}_{max}^\pi)_1$ is adjacent to two unsatisfied syndromes). If we save in \mathbf{w}_{hd} the set of variables that we have selected throughout this process, then the error candidate associated to \mathbf{w}_{hd} is guaranteed to match the syndrome in $O(n)$. Overall, forced convergence requires $O(n \log n)$.

Forced convergence is guaranteed to return an error

candidate with the observed syndrome. It is worth noting that, if marginalization converges, then forced convergence will output the same error candidate as marginalization. That is, if we converge we do not need to perform forced convergence and, thus, we can save computational time by checking for marginalization convergence before performing forced convergence. Fig. 2 is an example where marginalization does not converge and forced convergence does. Forced convergence is related to **guided decimation** [26].

III. RESULTS

The core of our results are two BP-based algorithms: BP4M, BP4MF. Additionally, we build also a two-stage decoder BP4M+M(atching). Since they all perform message-passing, their complexity and performance depend on the number of iterations T they use. For each algorithm we will consider two different num-

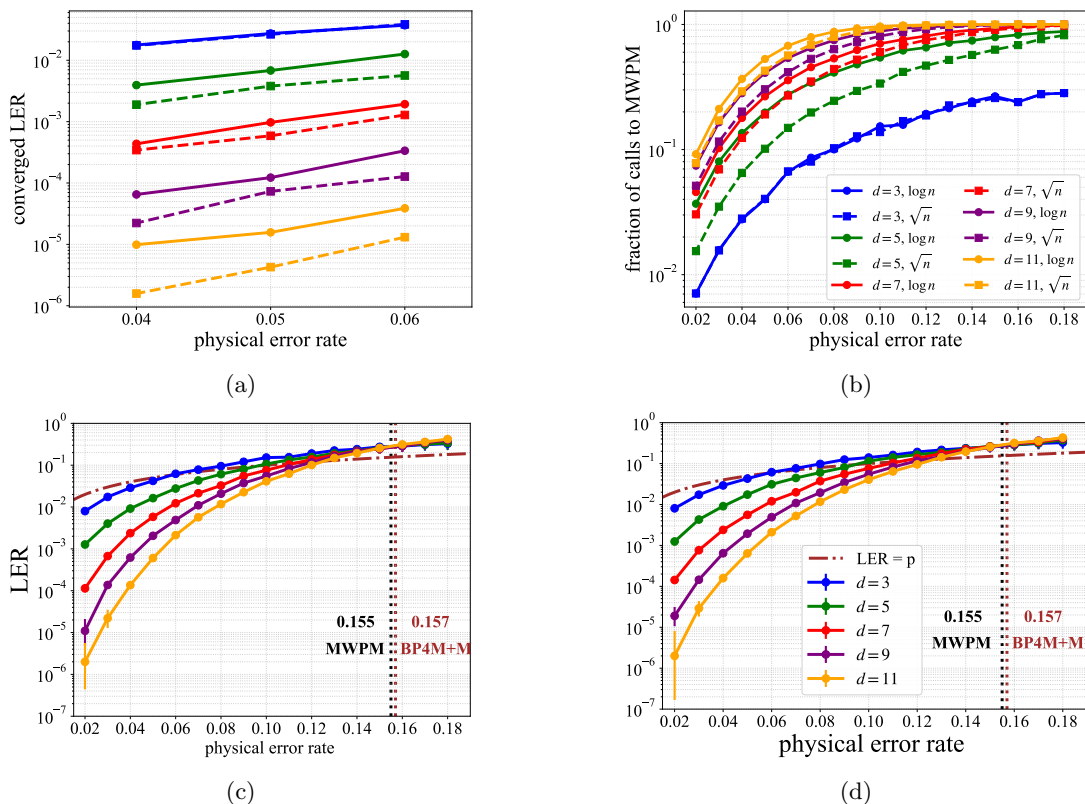


FIG. 4: Convergence performance and MWPM postprocessing: of message-passing without forcing convergence: (a) Converged LER. (b) Convergence fraction. (c) Performance BP4M+M- $\log n$. (d) Performance BP4M+M- \sqrt{n} .

ber of iterations $T = \log n, \sqrt{n}$, obtaining six algorithm instances: BP4M- $\log n$, BP4M- \sqrt{n} , BP4MF- $\log n$, BP4MF- \sqrt{n} , BP4M+M- $\log n$ and BP4M+M- \sqrt{n} . Table I lists the complexity of each algorithm.

A. Belief Propagation for Matching (BP4M)

Our first method is **belief propagation for matching (BP4M)**. Herein, we perform message-passing for a number of iterations T , performing marginalization at each iteration and, provided we converge in several iterations, keeping the error candidate with lowest weight among them. Once the iterations are over, we perform forced convergence in order to get some error candidate for each syndrome. Lastly, we compare the weight of the lowest candidate coming from marginalization with that of forced convergence and output the error candidate with smallest weight between them.

The complexity of each iteration of BP4M is that of message-passing itself $O(n)$ plus that of the marginalization $O(1)$ for a total of $O(nT)$ when finishing the iterations. After that, forced convergence requires $O(n \log n)$, and we get an overall complexity of $O(nT + n \log n)$. That is, the complexities of BP4M- $\log n$ and BP4M- \sqrt{n} are $O(n \log n)$ and $O(n^{3/2})$, respectively.

B. BP4M Forced (BP4MF)

The second method is called **belief propagation for matching forced (BP4MF)**. In this approach, we perform message-passing for a number of iterations T , performing forced convergence at each iteration and keeping the error candidate with lowest weight among them. For the same number of iterations T , we expect this approach to perform better than BP4M, since the weight of the final output will be upper bounded by that of BP4M. This is the case since, if marginalization converges, then forced convergence will output the same error candidate.

The complexity of each iteration of BP4MF is that of message-passing itself $O(n)$ plus that of forced convergence $O(n \log n)$ for a total of $O(n \log(n)T)$ when finishing the iterations. That is, the complexities of BP4MF- $\log n$ and BP4MF- \sqrt{n} are $O(n(\log n)^2)$ and $O(n^{3/2} \log n)$, respectively. Before performing forced convergence, we can marginalize and check for convergence for $O(n)$, and avoid the $O(n \log n)$ cost of forced convergence. The number of times forced convergence cannot be avoided diminishes with the physical error rate.

C. BP4M + Matching (BP4M+M)

The third method is **belief propagation for matching plus matching (BP4M+M)**. This is a two-stage decoder, where the first stage is running BP4M and the second one vanilla MWPM. In this approach, we reproduce BP4M while we are performing iterations and, once we have reached T iterations, we check whether we have converged. If that is the case, then we output the converged error candidate with minimal weight like BP4M does. Otherwise, we perform MWPM. This method is somehow similar to [27], although the soft information from BP4M is not used to reweigh the MWPM graph.

The complexity of each iteration of BP4M+M is that of BP4M, that is, $O(nT)$. If we do not obtain an error candidate that matches the observed syndrome after T iterations, then we use matching for an extra complexity of $O(n^3 \log n)$. As a result, if we call r_{nc} the **ratio of non-convergence**, i.e. the quotient of the number of times we do not converge and the number of errors we have generated, then the expected runtime is $O((1 - r_{nc})nT + r_{nc}n^3 \log n)$. That is, the complexities of BP4M+M- $\log n$ and BP4M+M- \sqrt{n} are $O((1 - r_{nc})n \log n + r_{nc}n^3 \log n)$ and $O((1 - r_{nc})n^{3/2} + r_{nc}n^3 \log n)$, respectively. As we show in Fig. 4b, r_{nc} diminishes with the physical error rate and we get for $p = 0.02$ that $r_{nc} \leq 0.1$ for $d = 3, 5, 7, 9, 11$.

D. Numerical Results

We benchmark using the unrotated surface code with distances $d = 3, 5, 7, 9, 11$. We consider code capacity noise under the depolarizing channel with physical error rates $p = 0.02, \dots, 0.18$. For comparison against vanilla MWPM we select PyMatching [22]. In addition, the MWPM subroutine within our BP4M+M decoder is also implemented using PyMatching. We have also used the QECSIM library [28].

We implemented our code with Numpy and C++. Simulations were performed on a Linux workstation running Ubuntu 24.04.3 LTS (kernel 6.8.0-94-generic), equipped with an AMD EPYC 9274F (24 cores / 48 threads, single socket; up to 4.05 GHz) and 188 GB RAM, and 2× NVIDIA RTX 6000 Ada Generation GPUs (48 GB VRAM each).

Our key numerical findings are the following:

- All of our algorithms have thresholds comparable to that of MWPM (Fig. 3, 4c and 4d, and Table I).
- All of our algorithms show good performance.

One can see this in Fig. 5 for $d = 9, 11$. As expected, for the same number of iterations T , we get that BP4MF- T performs better than BP4M- T .

- Adding complexity does not necessarily improve performance.

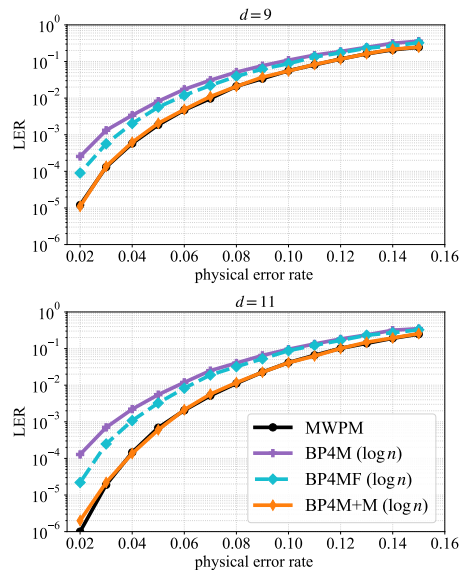


FIG. 5: Performance of our algorithms with $\log n$ iterations compared to MWPM for distances $d = 9, 11$.

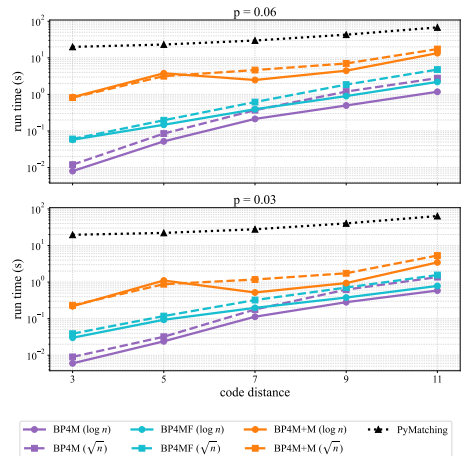


FIG. 6: Average runtimes (over 100 million errors) compared to MWPM.

Fig. 5 illustrates that despite being less complex, BP4MF- $\log n$ performs better than BP4MF- \sqrt{n} . This shows that even in the intermediate iterations where we do not converge, forced convergence provides meaningful error candidates. Moreover, exploring more of these candidates is more important in terms of performance than running more iterations and only exploring the converged error candidates.

- When we converge via marginalization, the performance is comparable to that of MWPM.

The performance of BP4M+M (Fig. 4c, 4d) is almost indistinguishable from that of MWPM even with $\log n$ message-passing iterations (Fig. 5). This indicates that, when our algorithms converge via

marginalization, their performance is comparable to that of MWPM. To support this, we include in Fig. 4a the **converged logical error rate** or **converged LER**, which consists of the logical errors ignoring the cases where we do not converge.

- The number of instances where we do not converge via marginalization diminishes with the physical error rate (Fig. 4b).
- A low number of iterations is sufficient.

Fig. 5 shows that running the same algorithm with \sqrt{n} iterations does not result in a huge performance gain compared to running $\log n$ iterations. For BP4M, we only notice the difference in performance for low physical error rates. For BP4MF, the difference in performance is already present for high physical error rates, but it is not large. For BP4M+M, the performance of both methods is essentially the same, with BP4M+M- $\log n$ requiring more calls to MWPM (Fig. 4b).

- We achieve a faster runtime compared to MWPM (Fig. 6).

IV. CONCLUSION

We have demonstrated that standalone belief propagation (BP), in the form of the BP4M algorithm, can achieve code capacity thresholds for the surface code under depolarizing noise by shifting message-passing from the Tanner graph to the decoding graph. Our proposed algorithms yield thresholds comparable to minimum weight perfect matching (MWPM). In order to achieve competitive LER for higher distances we introduced a forced convergence strategy which we called BP4MF. Furthermore, when used as a pre-decoder for MWPM, our approach speeds-up the decoding significantly because of its high convergence ratio. Additionally, we found that a low number of iterations is sufficient for high performance, and forced convergence techniques effectively ensure valid error candidates even when standard marginalization fails. Future research will focus on benchmarking these methods under circuit-level noise. Another interesting direction is to use the output of vanilla BP in order to update the prior probabilities in our algorithms, in the spirit of BP-matching [27].

ACKNOWLEDGEMENTS

We thank Francisco García Herrero for feedback on the manuscript and Henry D. Pfister for useful discussions. This research was supported by the Munich Quantum Valley. The research is part of the Munich Quantum Valley, which is supported by the Bavarian state government with funds from the Hightech Agenda Bayern P.

-
- [1] E. Dennis, A. Kitaev, A. Landahl, and J. Preskill, Topological quantum memory, *Journal of Mathematical Physics* **43**, 4452 (2002).
 - [2] N. P. Breuckmann and B. M. Terhal, Constructions and noise threshold of hyperbolic surface codes, *IEEE transactions on Information Theory* **62**, 3731 (2016).
 - [3] S. Bravyi, G. Duclos-Cianci, D. Poulin, and M. Suchara, Subsystem surface codes with three-qubit check operators, *arXiv preprint arXiv:1207.1443* (2012).
 - [4] M. Suchara, S. Bravyi, and B. Terhal, Constructions and noise threshold of topological subsystem codes, *Journal of Physics A: Mathematical and Theoretical* **44**, 155301 (2011).
 - [5] D. Bacon, Operator quantum error-correcting subsystems for self-correcting quantum memories, *Physical Review A—Atomic, Molecular, and Optical Physics* **73**, 012340 (2006).
 - [6] M. B. Hastings and J. Haah, Dynamically generated logical qubits, *Quantum* **5**, 564 (2021).
 - [7] H. Bombin and M. A. Martin-Delgado, Topological quantum distillation, *Physical review letters* **97**, 180501 (2006).
 - [8] A. Kubica and N. Delfosse, Efficient color code decoders in $d \geq 2$ dimensions from toric code decoders, *Quantum* **7**, 929 (2023).
 - [9] B. J. Brown, Conservation laws and quantum error correction: Toward a generalized matching decoder, *IEEE BITS the Information Theory Magazine* **2**, 5 (2023).
 - [10] A. G. Fowler, Minimum weight perfect matching of fault-tolerant topological quantum error correction in average $o(1)$ parallel time, *arXiv preprint arXiv:1307.1740* (2013).
 - [11] N. Delfosse and N. H. Nickerson, Almost-linear time decoding algorithm for topological codes, *Quantum* **5**, 595 (2021).
 - [12] O. Higgott and C. Gidney, Sparse blossom: correcting a million errors per core second with minimum-weight matching, *Quantum* **9**, 1600 (2025).
 - [13] K.-Y. Kuo and C.-Y. Lai, Refined belief propagation decoding of sparse-graph quantum codes, *IEEE Journal on Selected Areas in Information Theory* **1**, 487 (2020).
 - [14] Y.-H. Liu and D. Poulin, Neural belief-propagation decoders for quantum error-correcting codes, *Physical review letters* **122**, 200501 (2019).
 - [15] A. deMartini, P. Fuentes, R. Orús, P. M. Crespo, and J. E. Martinez, Decoding algorithms for surface codes, *Quantum* **8**, 1498 (2024).

- [16] M. Bayati, D. Shah, and M. Sharma, Maximum weight matching via max-product belief propagation, in *Proceedings. International Symposium on Information Theory, 2005. ISIT 2005.* (IEEE, 2005) pp. 1763–1767.
- [17] S. Sanghavi, D. Malioutov, and A. Willsky, Linear programming analysis of loopy belief propagation for weighted matching, *Advances in neural information processing systems* **20** (2007).
- [18] M. Bayati, D. Shah, and M. Sharma, Max-product for maximum weight matching: Convergence, correctness, and lp duality, *IEEE Transactions on information theory* **54**, 1241 (2008).
- [19] A. E. Gelfand, J. Shin, and M. Chertkov, Belief propagation for linear programming, in *2013 IEEE International Symposium on Information Theory* (IEEE, 2013) pp. 2249–2253.
- [20] S.-S. Ahn, S. Park, M. Chertkov, and J. Shin, Minimum weight perfect matching via blossom belief propagation, *Advances in neural information processing systems* **28** (2015).
- [21] J. Edmonds, Paths, trees, and flowers, *Canadian Journal of mathematics* **17**, 449 (1965).
- [22] O. Higgott, Pymatching: A python package for decoding quantum codes with minimum-weight perfect matching, *ACM Transactions on Quantum Computing* **3**, 1 (2022).
- [23] M. Mezard and A. Montanari, *Information, physics, and computation* (Oxford University Press, 2009).
- [24] D. S. Wang, A. G. Fowler, A. M. Stephens, and L. C. Hollenberg, Threshold error rates for the toric and surface codes, arXiv preprint arXiv:0905.0531 (2009).
- [25] D. Bascones and B. Morcillo, Hourglass sorting: A novel parallel sorting algorithm and its implementation, arXiv preprint arXiv:2507.16326 (2025).
- [26] H. Yao, W. A. Laban, C. Häger, A. G. i Amat, and H. D. Pfister, Belief propagation decoding of quantum ldpc codes with guided decimation, in *2024 IEEE International Symposium on Information Theory (ISIT)* (IEEE, 2024) pp. 2478–2483.
- [27] O. Higgott, T. C. Bohdanowicz, A. Kubica, S. T. Flammia, and E. T. Campbell, Improved decoding of circuit noise and fragile boundaries of tailored surface codes, *Physical Review X* **13**, 031007 (2023).
- [28] D. K. Tuckett, *Tailoring surface codes: Improvements in quantum error correction with biased noise*, Ph.D. thesis, University of Sydney (2020), (qecsim: <https://github.com/qecsim/qecsim>).